Title Page

Filovirus antiviral activity of cationic amphiphilic drugs is associated with lipophilicity and ability to induce phospholipidosis

Authors and affiliations:

Antonia P. Gunesch[a,b,c], Francisco J. Zapatero-Belinchon[a,b,c] , Lukas Pinkert[d], Eike Steinmann[e], Michael P. Manns[a,b], Gisbert Schneider[f], Thomas Pietschmann[b,c], Mark Brönstrup[b,d], Thomas von Hahn[a,b,c,g#]

a. Department of Gastroenterology, Hepatology and Endocrinology, Hannover Medical School, Hannover, Germany
b. German Center for Infection Research (DZIF), Hannover-Braunschweig site, Germany;
c. Institute of Experimental Virology, TWINCORE, Center for Experimental and Clinical Infection Research Hannover, Hannover, Germany
d. Department of Chemical Biology, Helmholtz Centre for Infection Research (HZI), Braunschweig, Germany
e. Department for Molecular & Medical Virology, Ruhr-Universität Bochum, Bochum, Germany
f. Department of Chemistry and Applied Biosciences, Institute of Pharmaceutical Sciences, Eidgenössische Technische Hochschule (ETH) Zürich, Switzerland
g. Department of Gastroenterology and Interventional Endoscopy, Asklepios Hospital Barmbek, Semmelweis University, Campus Hamburg, Germany

#Corresponding author: Prof. Dr. med. Thomas von Hahn, t.hahn@asklepios.com.

Short running title: Antiviral structure-activity relationship of cationic amphiphilic drugs

1. Abstract

Several cationic amphiphilic drugs (CADs) have been found to inhibit cell entry of filoviruses and other enveloped viruses. Structurally unrelated CADs may have antiviral activity, yet the underlying common mechanism and structure-activity relationship are incompletely understood.

We aimed to understand how widespread antiviral activity is among CADs and which structural and physico-chemical properties are linked to entry inhibition.

We measured inhibition of Marburg virus pseudoparticle (MARVpp) cell entry by 45 heterogeneous and mostly FDA-approved CADs and cytotoxicity in EA.hy926 cells. We analysed correlation of antiviral activity with four chemical properties: pKa, ClogP, molecular weight and distance between the basic group and hydrophobic ring structures. Additionally, we quantified drug-induced phospholipidosis (DIPL) of a CAD subset by flow cytometry. Structurally similar compounds (derivatives) and those with similar chemical properties but unrelated structure (analogues) to strong inhibitors were obtained by two *in silico* similarity search approaches and tested for antiviral activity. Overall 11 out of 45 (24 %) CADs inhibited MARVpp by 40 % or more. The strongest antiviral compounds were dronedarone, triparanol and quinacrine. Structure-activity relationship studies revealed highly significant correlations between antiviral activity, hydrophobicity (ClogP>4), and DIPL. Moreover, pKa and intra-molecular distance between hydrophobic and hydrophilic moieties correlated with antiviral activity, but to a lesser extent. We also showed that in contrast to analogues, derivatives had similar antiviral activity as the seed compound dronedarone. Overall, one quarter of CADs inhibits MARVpp entry *in vitro* and antiviral activity of CADs mostly relies on their hydrophobicity, yet is promoted by the individual structure.

2. Introduction

Outbreaks of emerging viral diseases have repeatedly posed major challenges to global health in the recent years (https://www.who.int/csr/don/en/). Important examples include the *Filoviridae* Ebola virus (EBOV) and Marburg virus (MARV), *Arenaviridae* Lassa virus (LASV), *Coronaviridae* like Middle East Respiratory Syndrome coronavirus (MERS-CoV), or the *Flaviviridae*-member ZIKA. Some of these infections are associated with high case-fatality rates, e.g. 50 % for EBOV and MARV, 35 % for MERS-CoV (2), and up to 30 % for hospitalized LASV patients (3). Thus according to the *WHO-List of Blueprint priority diseases* of 2018, the aforementioned pathogens share priority status concerning the need for research and development given that effective vaccines or direct acting antivirals are unavailable in most cases (4). It would be of great value to have drugs that are active against a broad range of viral pathogens (5, 6). Such agents would likely not target specific components of individual viruses but rather cellular structures or processes that are utilized by various unrelated viruses. An attractive target pathway concerns cellular endosomal processes, since these are used by numerous pathogens including members of the families *Filoviridae, Arenaviridae*, *Rhabdoviridae*, *Coronaviridae*, *Togaviridae*, *Flaviviridae* and *Bunyaviridae.*

Cationic amphiphilic drugs (CADs) are a diverse group of compounds, many of which are in medical use for various clinical indications. CADs are defined by a hydrophilic group marked by a basic amine with high pKa (the negative logarithm of the acid dissociation constant Ka) and hydrophobic group(s) characterised by several aromatic or aliphatic structures (7). Due to their amphiphilic nature CADs transmigrate membranes which can be enhanced by different substituents like halogen residues. Upon reaching acidic compartments like late endosomes (LE) and endolysosomes, the basic amine groups gets protonated, which leads to lysosomal

trapping of the compounds (8). Consequently, CADs primarily accumulate in acidified compartments (9, 10).

Several studies, most of which analysed sets of approved drugs, have found that various CADs have antiviral activity. The antiarrhythmics amiodarone, dronedarone and verapamil (11) as well as the estrogen receptor antagonists clomifene and toremifene (12) have been shown to inhibit filoviral entry in different cell lines. Moreover, clomifene and toremifene were shown to elevate survival rates of mice infected with mouse-adapted EBOV up to 90% (12). Of note, they could show that the antiviral activity of these two CADs was unrelated to their clinical mechanism of action as estrogen receptor modulators. Beyond filoviruses, CADs have also been found to inhibit *Arenaviridae* LASV and Guanarito virus (GTOV) (13), Hepatitis C virus (HCV) (14–18), Japanese encephalitis virus (JEV) (19), Severe acute respiratory syndrome-related coronavirus (SARS-CoV) (20), and Eppstein-Barr virus (EBV) (21). Moreover, it was found that the CADs amiodarone, bepridil, raloxifene and amodiaquine besides several non-CAD compounds have broad antiviral effects against all tested alpha- and flaviviruses (with the exception of ZIKA virus), as well as varying other viruses, but none inhibited Human immunodeficiency virus (HIV) (22). Highest antiviral activity for all four CADs was found against EBOV virus like particles. Despite these observations, it is not known so far how widespread antiviral activity really is among CADs. Likewise, the mechanism of action behind the antiviral activity is unclear. For this reason, we undertook a comprehensive study of antiviral acitivity among 45 heterogeneous CAD compounds and correlated antiviral activity with various physico-chemical properties.

3. Material and Methods

2.1 Pseudoparticle production and transduction

Pseudoparticles were produced as described before (23, 24). In brief, producer HEK-293T cells were seeded at $8*10^5$ cells/well in a poly-L-lysine coated 6-well plate. After 24 h cells were co-transfected with 1 µg DNA using polyethyleneimine (PEI) to produce HIV-based pseudoparticles bearing individual viral envelope gp. The plasmids used were (1) a packaging plasmid containing HIV-based gag-pol genes (25), (2) a plasmid encoding for the *env* gene of MARV (pCAGGS-MARVGP) (26) or an empty vector pcDNA3.1 and (3) a gutted yet packaging competent HIV-based transfer plasmid encoding for NLuc reporter gene (pWPI_NanoLuc_BLR) (in a ratio 1:1:4). After 6 h post-transfection, medium was exchanged for 3 % FCS DMEM containing 5 % Penicillin/Streptomycin and pseudoparticles harvested, pooled and filtered after 48 h and 72 h. For lentiviral transduction, target EA.hy926 cells were seeded $1*10^4$ cells / well in a 96-well plate. After incubation for 24 h, 50 µL of MARVpp or 50 µL complete DMEM were mixed with polybrene (1:1000) and CADs to an end-concentration of 5 µM and applied in triplicates. As a solvent control sterile water, EtOH, or DMSO were diluted in DMEM complete in the same ratio as the drugs. At 6 h post transduction (h.p.t), cells were washed once with phosphate buffered saline (PBS) and 100 µL of complete DMEM were applied. Seventy-two h.p.t, cells were washed with PBS and lysed. Next, 20 µL of cell lysate were transferred to a 96-well luminometer plate, mixed with 80 µL of the luciferase substrate coelenterazine, and incubated shortly in the dark before NLuc activity quantification in a GloMax® plate luminometer (Promega, Madison, WI, USA), representing gp-driven cell entry.

2.2 Cytotoxicity test

EA.hy926-NLuc were seeded at $1*10^4$ cells/well in a 96-well plate. The next day, cells were treated in triplicate with either complete DMEM, solvent control (complete DMEM + solvent), or with diluted CADs at a final concentration of 5 µM. After 6 h, cells were washed with PBS and incubated with 100 µL complete DMEM for another 72 h at 37 C. Then cells were lysed and luciferase activity was determined as an aggregate measure of cell viability and proliferation.

Compounds and similarity search

The compounds amiodarone HCl (A8423), amorolfine HCl (SML0283), bepridil HCl (B5016), clemastine fumarate salt (SML0445), clomiphene citrate salt (C6272), dasatinib (CDS023389), dronedarone HCl (D9696), perhexiline maleate salt (SML0120), promazine HCl (P6656), sertraline HCl (S6319), terconazole (32355), toremifene citrate salt (T7204), triparanol (T5200), chlorcyclizine (SML1473), clozapine (C6305), cyclizine HCl (C3090000), N-Desethylamiodarone HCl solution (D-055), verapamil HCl (V4629), W-7 (N-(6-Aminohexyl)-5-chloro-1-naphthalenesulfonamide hydrochloride) (A3281), amantadine HCl (A1260), Benzylamine (185701), chloroquine diphosphate salt (C6628), clomipramine HCl (C7291), chlorpromazine HCl (C0982), enclomiphene HCl (SML0719), fenfluramine HCl (F112), flupentixol dihydrochloride (Y0000064), fluphenazine dihydrochloride (F4765), gentamicin sulfate (G1914), imipramine HCl (I0899), maprotiline HCl (M9651), mianserin HCl (M2525), prochlorperazine dimaleate salt (P9178), promethazine HCl (P4651), propranolol HCl (P0884), quinacrine dihydrochloride (Q3251), teicoplanin (T0578), thioridazine HCl (T9025), trifluoperazine HCl (T6062), tripelennamine HCl (T7511), U18666A (U3633), W-5 (N-(6-Aminohexyl)-1-naphthalenesulfonamide hydrochloride) (SML0657), zimelidine dihydrochloride

(Z101) were purchased from Sigma-Aldrich Chemie GmbH (Taufkirchen, Germany). The compound Ro 48-8071 was purchased from Biomol GmbH (Hamburg, Germany).

Dronedarone-derivatives were received using SciFinder® software (Chemical Abstracts Service, 2017). D-1 (N-Mesyldronedarone; TRC-M225785) and D-2 (S-Desmethyl S-Chloromethyl Dronedarone; TRC-D291470) were purchased from BIOZOL Diagnostica Vertrieb GmbH (Eching, Germany). To obtain analogous CADs, chemical advanced template search (CATS) software was used (Schneider et al., 1999). The compounds AC1 (1-(4-Ethyl-1-piperazinyl)-4-[1-(4-methylbenzyl)-1H-indol-3-yl]-1-butanone; E230-0651), CS3 (2-[(E)-2-{4-[Ethyl(4-methoxyphenyl)amino]phenyl}vinyl]-3-methyl-1.3-benzothiazol-3-ium; 7165-0012) and QT1 (G119-1593; G119-1593) were obtained by ChemDiv (San Diego, CA, USA). CS1 (2-{2-[(3.4-dichlorophenyl)thio]ethyl}-1-(2-oxo-2-phenylethyl)pyridinium bromide; 5841320) and CS2 (1-{2-[4-(1-methyl-1-phenylethyl)phenoxy]ethyl}pyrrolidine; 7020606) were ordered from ChemBridge Corporation (San Diego, CA, USA). DQ1 (2-(4-(sec-butyl)phenyl)-N'(1-phenethylpiperidin-4-ylidine)quinolone-4-carbohydrazide; IVK 9315735) was purchased from SRC Alinda (Moscow, Russia) and CS4 (5-bromo-2-{[1-(3-fluorophenyl)ethyl]sulfanyl}pyridine; PB742999078) from Chemspace (Riga, Latvia). CT1 ((E)-1-(5-chlorothiophen-2-yl)-3-(4-(diphenylamino)phenyl)prop-2-en-1-one; Z46049784) was purchased from Enamine (Monmouth junction, NJ, USA). As solvents water, ethanol (EtOH) (Carl Roth, Karlsruhe, Germany), or dimethylsulfoxid (DMSO) (Carl Roth, Karlsruhe, Germany), were used.

178 *Cell culture*

179 Immortalized epithelial HEK-293T and EA.hy926, a fusion product of A549 and
180 human umbilical vein endothelial cells, were cultured in Dulbecco's Modified Eagle
181 medium (DMEM) with 10 % fetal calf serum (FCS), 5 % Penicillin/Streptomycin, 5 %
182 non-essential aminoacids (NEAA) and 5 % L-glutamine (complete DMEM) at 37 °C
183 with 5 % CO_2. Luciferase-expressing EA.hy926-NLuc cells were obtained by
184 transduction with VSV-Gpp harboring the nano luciferase (NLuc) gene and cultured
185 as previously described.

186

187 *Phospholipidosis assay*

188 EA.hy926 cells were seeded at $1*10^4$ cells/well in a 96-well plate. The next day,
189 CADs and their solvents (DMSO and water) were diluted in culture medium.
190 Phospholipidosis was quantified using LipidTOX™ Green Phospholipidosis Detection
191 Reagent (H34350, Thermo Fisher Scientific, Waltham, MA, USA) according to a
192 modified version of a degradation assay (Mesens et al., 2009). In brief, LipidTOX™
193 was diluted 1:500 in complete DMEM and sterile filtered. Then 50 µL of either CAD
194 mixture or controls were applied to the cells together with 50 µL of diluted LipidTox,
195 resulting in a final CAD concentration of 5 µM and a final LipidTox dilution of 1:1000.
196 After incubation for 6 h at 37 °C, cells were washed once with PBS. Medium was
197 exchanged for 100 µL culture medium and only the drugs (5µM) but no LipidTOX™
198 were added a second time. After 24 h in total, cells were washed with PBS,
199 trypsinised, and transferred to FACS tubes. Cells were washed with 1 mL FACS
200 buffer (2 % FCS in PBS), centrifuged for 5 min at 1000 rpm and supernatant
201 discarded. In some replicates, cells were fixed with 100 µL 3-6 % PFA with no
202 influence on the results. Finally, CAD-induced lysosomal accumulation of LipidTOX™
203 was quantified as intracellular green fluorescence by flow cytometry in BD

FACSCanto II (BD, Franklin Lakes, NJ, USA) or for derivates in Spectral Cell Analyzer SA3800 (Sony Biotechnology, San Jose, CA, USA) and analysed with FlowJo V9 and V10.

Chemical properties / parameters

The chemical parameters of CADs including molecular weight, pKa and octanol/water partitioning coefficient (ClogP) were obtained from either the respective data sheets or the databases Pubchem (Kim et al., 2019), drugbank (Wishart et al., 2018) and ChemDraw Professional 18 (PerkinElmer, Hamburg, Germany). The parameter "linker length" was defined as the distance between the amine group and the first hydrophobic ring structure. We determined linker length by compiling the 3D structure of each CAD in Chem3D Pro 18 (PerkinElmer, Hamburg, Germany), performed a MM2 energy minimization and then used coordinates x, y and z of the amine and hydrophobic group to calculate the distance.

Statistical analysis

Unless stated otherwise, experiments were conducted three times in triplicate. Statistical analysis was performed in GraphPad Prism 7 (La Jolla, CA, USA). The statistical significance between multiple groups and the control groups was evaluated by ordinary One-way ANOVA followed by multiple comparisons test (Dunnett) and for correlation analyses a non-parametric Spearman-correlation was run. Concentration-response curves were fitted by non-linear regression ([Inhibitor] vs. response - variable slope (four parameters)) and IC50 and CC50 values interpolated from the resulting standard curve.

4. Results

3.1 Side-by-side assessment of MARV gp-driven cell entry inhibition and cytotoxicity of 45 CADs

We firstly attempted to evaluate how common antiviral activity is among CADs. Therefore, we selected an initial set of 45 CADs (Table 1) based on the following criteria: (i) coverage of multiple drug classes, (ii) diverse chemical structures aside from being CADs, (iii) preferentially FDA- or EMA-approved compounds / no known major toxicity and (iv) commercial availability. We included CADs that have either previously been reported to have antiviral activity or are known to cause drug-induced phospholipidosis (DIPL).

In order to test many drugs at the same time, a single-point 96-well assay was established, that enabled testing the entire set of compounds at the same micromolar concentration against a high-titer preparation of lentiviral particles pseudotyped with the MARV gp (MARV pseudovirus, MARVpp) in endothelium-derived EA.hy926 cells. Beforehand, we conducted concentration-response and -toxicity curves of the prototypical, antivirally active CAD amiodarone in EA.hy926 cells against MARVpp. The half-maximal inhibitory (IC_{50}) and cytotoxic (CC_{50}) concentrations were IC_{50} = 1.6 µM and CC_{50} = 54 µM, respectively (Figure S1). Consequently, we chose a test concentration of 5 µM for all CADs, i.e. 2.8-fold above the IC_{50} and almost 10-fold below the CC_{50} of amiodarone.

The ability to inhibit MARVpp entry in EA.hy926 differed widely within the set of CADs tested (Figure 1a). Approximately 24 % of CADs showed antiviral activity (>40 % inhibition), with strongest effects by dronedarone and triparanol (>80 % inhibition), followed by >60 % inhibition of quinacrine, sertraline, amiodarone, perhexiline, clomifene and N-desethylamiodarone. Notably, cytotoxicity measurement in EA.hy-NLuc cells revealed that most CADs do not have major toxic effects on these cells.

256 However, treatment with dasatinib, quinacrine and sertraline showed a 42 %, 22 %
257 and 19 % reduction of viability, respectively (Figure 1b). Our results demonstrate that
258 antiviral activity is not a common feature of all CADs and independent of the drug
259 class.
260
261 **3.2 Determination of antiviral potency and safety of top and bottom CADs**
262 Next, we generated concentration-response curves for the six CADs that showed the
263 highest antiviral activity (dronedarone, triparanol, sertraline, amiodarone, perhexiline
264 and clomifene) (Figure S1) and for the six least antiviral CADs (propranolol,
265 tripelennamin, amantadine, promazine, zimelidine and benzylamine) (Figure S2).
266 Quinacrine and dasatinib were excluded from further analyses due to their high
267 cytotoxicity (Figure 1). Likewise, teicoplanin was excluded because its high molecular
268 size and structural complexity would hamper the structure-function analysis. The
269 determined IC_{50} and CC_{50} values as well as the selective indices (SI) are
270 summarised in Table 2. We observed that strong antiviral CADs act in a micromolar
271 concentration with IC_{50} values between 1.3 µM (dronedarone) and 2.9 µM (sertraline)
272 and CC_{50} between 13.2 µM (dronedarone) and 54 µM (amiodarone). In contrast,
273 weakly active CADs in most cases did not allow for IC_{50} and CC_{50} calculation except
274 for propranolol (IC_{50} 64.6 µM) and promazine (IC_{50} = 29.3 µM and CC_{50} = 51.6 µM).
275 Notably, we observed relatively narrow non-toxic activity windows, with the broadest
276 one for amiodarone (SI = 34), followed by clomifene (SI = 17), triparanol (SI = 13),
277 and dronedarone (SI = 10).
278
279 **3.3 Anti-MARVpp activity of CADs correlates with specific physico-chemical**
280 **properties and DIPL induction**

281 Next, we addressed the question whether strong antiviral activity of CADs was
282 associated with physico-chemical properties. Specifically, we correlated the CADs'
283 antiviral activity with their acidity (pK_a), hydrophobicity (ClogP), molecular weight
284 (MW) and the distance between hydrophilic amine and hydrophobic ring structure of
285 the molecules ('linker length') (Figure 2 a-d). The parameters pKa, ClogP and MW
286 were obtained mainly from databases, whereas the linker length was calculated
287 according to the 3D structure of the molecules. Although we could not observe any
288 correlation between antiviral activity and linker length (Figure 2 d), we noticed a
289 modest yet unsignificant ($R = -0.24$; $p = 0.11$) association of antiviral activity with
290 pKa, showing that more alkaline CADs have higher antiviral activity (Figure 2 a). We
291 observed similar correlation with molecular weight ($R = -0.33$; $p = 0.02$) (Figure 2 c).
292 Most strikingly, we found a highly significant correlation between antiviral activity and
293 hydrophobicity ($R = -0.78$; $p < 0.0001$) (Figure 2 b). Although the majority of CADs is
294 rather hydrophobic ($1 < ClogP < 8$), all strong antiviral CADs had a octanol/water
295 partitioning coefficient larger than four ($ClogP > 4$). Taken together, CADs with
296 $ClogP > 4$ and $pKa > 8$ are more likely to be antiviral.
297 Next, we analysed to what extent antiviral activity is associated with induction of DIPL
298 (Figure 3). Therefore, we treated EA.hy926 cells with 16 of the CADs at 5 µM or their
299 solvents, both in presence of LipidTox™. The latter is a fluorophore-conjugated
300 phospholipid which permeates cellular membranes, but is believed to be complexed
301 in endosomes upon DIPL induction. The selected CADs were chosen for their varying
302 degrees of antiviral activity against MARVpp and comprised of ten more or less
303 active CADs and six inactive CADs – thus, we aimed to represent the full spectrum of
304 antiviral acitivity seen with CADs. We detected green fluorescence as a measure for
305 lysosomal accumulation of LipidTox™, representing CAD-induced DIPL. Here, we
306 could not only show a highly significant correlation of MARVpp antiviral activity with

the degree of DIPL induction (R = -0.81; p = 0.0001) (Figure 3 a), but also significant association of DIPL-induction and hydrophobicity of these compounds (R = 0.73; p = 0.0011) (Figure 3 b). These findings underline the importance of hydrophobicity, mediating both antiviral activity and DIPL of CADs. Furthermore they hint that DIPL and antiviral activity might be more closely related than previously suggested.

3.4 Selection of additional CADs based on our previous findings and validation of their antiviral activity and cytotoxicity

We observed that strong antiviral activity in CADs is associated with certain physico-chemical features, yet antiviral CADs can vary widely in their scaffold structures. In order to gain an insight how far the chemical structure and/or chemical properties influence antiviral activity, we validated additional CADs that were identified by two distinct approaches.

First, we tested whether compounds with comparable molecular structure (derivatives) would have similar or even stronger antiviral effects than antiviral CADs. Dronedarone-derivatives (N-Mesyldronedarone (D-1) and S-Desmethyl S-Chloromethyl Dronedarone (D-2)) were obtained by a similarity search using SciFinder®, a curated chemistry information database (27). We thus analysed their antiviral activity against MARVpp gp-driven cell entry as well as their cytotoxicity in comparison to dronedarone and solvent (Figure 4 a, b). We found 94 % and 91 % inhibition for 5 µM D-1 and D-2, respectively. This is comparable to the antiviral effect seen with dronedarone itself and suggests that the CAD structure may be important for antiviral activity. Furthermore, we could show that these two compounds induce DIPL similarly to dronedarone (Figure S4). In line with our previous observations, D-1 and D-2 have a basic pKa and are highly hydrophobic with ClogP-values of 8.6 and 9.2, respectively.

As a second approach, we looked for chemically similar, but structurally diverse CADs (analogues) by chemically advanced template search (CATS) analysis (28). CATS largely disregards structural similarities and considers only similar chemical properties of compounds. As query substances, we submitted the seven most potent CADs amiodarone, dronedarone, triparanol, sertraline, quinacrine, perhexiline and clomifene. We found 33 new compounds that were identified as 'double hits' for showing functional similarity to two unrelated seed CADs. As we were aiming for putative antiviral candidates and in accordance with the observed importance of hydrophobicity for antiviral effective CADs, we further narrowed the number of hits down to compounds with ClogP > 4. By further selecting for diverse functional groups we obtained a set of eight compounds and named them according to the two seed compounds they derive from. We tested their antiviral activity against MARVpp as wells as cytotoxicity (Figure 5 a, b) and found that the compounds CT1, CS3, AC1, CS1, CS2 and QT1 decreased MARVpp entry (inhibition ranged from 17 % - 45 %). Still, the newly identified compounds did not reach the level of inhibition seen with their respective seed compounds.

5. Discussion

This study is to date the most comprehensive evaluation of both the distribution of antiviral activity among different types of CADs as well as their antivirally relevant physico-chemical properties. It reveals that: (1) Antiviral activity is not universal among CADs, but limited to a minority. (2) Antiviral CADs come from a broad range of pharmacological classes and have diverse molecular structures. (3) Certain physico-chemical features are associated with antiviral activity, most notably hydrophobicity. (4) There is a strong association between antiviral activity, the ability to induce cellular phospholipidosis and hydrophobicity.

358 Previous studies showed that amiodarone, as well as its close relative dronedarone
359 act in low micromolar concentrations against pseudoparticles of different filovirus
360 species, GTOV and influenza H5N1. Furthermore, amiodarone was shown to inhibit
361 authentic EBOV, HCV, SARS and recently semliki forest virus, dengue virus, Sindbis
362 virus, Ross river virus, herpes simplex virus and the attenuated vaccine strain of
363 yellow fever virus. Conversely, ZIKV, HIV or vaccinia virus were not affected. (14, 15,
364 20, 22, 29–31) Triparanol was found to inhibit EBOV VLP as well as EBOV infection
365 and HCV replication (17, 32). Among a variety of other CADs, quinacrine, sertraline
366 and clomifene inhibited mainly EBOV VLPs, mouse-adapted EBOV and other
367 filovirus strains, including MARV (12, 33). To our knowledge, perhexiline has not
368 been investigated in the context of antivirals yet and was included in our study due to
369 reported association with DIPL (8). Furthermore, the amiodarone metabolite mono-N-
370 desethylamiodarone (MDEA) was shown to have additive effects with amiodarone
371 (30). With our results, we partially confirmed and extended the previous studies.
372 Notably, we could show that the drugs dronedarone and triparanol followed by
373 quinacrine, sertraline, amiodarone, perhexiline, clomifene and N-desethylamiodarone
374 have higher antiviral potential within the broad field of described CADs. Furthermore,
375 we show that candidates previously not associated with antiviral effects but only with
376 DIPL (e.g. perhexiline) may also be potent antivirals or templates for further drug
377 development. Experiments were performed in the endothelium/lung-hybrid cell line
378 EA.hy926 that is easy to cultivate and gives low background. Besides monocytes,
379 macrophages, endothelial cells, hepatocytes and fibroblasts, this cell line was shown
380 to be susceptible to several enveloped viruses including filoviruses (11, 13, 34, 35).
381 Concentration-response analyses showed that the six strongest CADs act at low
382 micromolar concentrations. The IC_{50} values for amiodarone and sertraline are
383 comparable to the reported plasma concentrations ($C_{max(amiodarone)}$ = 1.5 – 2.5 mg/L

(2.2 – 3.7 µmol/L) and $C_{max(sertraline)}$ = 0.352 µmol/L, which can accumulate up to 20-fold in the liver (36–38). In case of dronedarone, the determined IC_{50} value is 10-fold higher than the plasma concentration achieved in treatment of arrhythmia ($C_{max(dronedarone)}$ = 84 – 147 µg/L (0.14 – 0.25 µmol/L)) (39). The selectivity index of these CADs is relatively narrow *in vitro*. However, it may be worth to probe whether a therapeutic window exists in vivo, which might be acceptable when dealing with a severe or even life-threating disease or in an outbreak setting triggered by emerging enveloped viruses, given that they act against a range of viruses.

In a previous study, Shoemaker et al. identified six highly antiviral CADs among various sterol pathway inhibitors. These CADs were characterized with a positively charged amine group, alkaline pKa (> 8.8), small MW, high hydrophobicity, and they caused cholesterol accumulation (32). However, it is not known whether the previous observations apply necessarily to all antivirally active CADs and which set of structural features define antiviral activity. To understand the relationship between CAD structure and antiviral activity we initially focused on a limited number of properties including pKa, ClogP, MW, and linker length. Hydrophobicity is an important determinant of membrane permeability and bioavailability of a molecule, and has been described as one of the key factors for ligand binding together with molar refractivity and formal charge density (8, 40, 41). We could show that strongly hydrophobic compounds have significantly stronger capacity to inhibit viral entry. The reason for this observation is so far unclear, but it may suggest that CADs need to be able to traverse membranes in order to exert their antiviral effect. Apart from the CAD-determining amine and hydrophobic groups, we were not able to identify a set of functional groups that is required for antiviral activity.

We further analysed CADs with either structural (derivatives) or functional (analogues) similarity to strong antiviral CADs of our screen (28, 42). The fact that

410 only the derivatives, but none of the analogues reached the level of inhibition seen
411 with their respective seed compounds suggests that structural architecture seemed to
412 have more impact on the CADs activity than chemical properties only. Nevertheless,
413 the analogues' activity rate is far higher than the one obtained by screening random
414 collections. However, these data show that hydrophobicity alone is not a certain
415 predictor for antiviral activity, but rather a combination of chemical properties, which
416 is also suggested for DIPL-induction (43, 44). An extended multiparametric analysis
417 would be useful to identify a larger set of (interdependent) parameters that enable
418 and enhance activity (28).
419 In addition, our studies showed a strong association between CAD antiviral activity
420 and the ability to induce DIPL in target cells, i.e. lysosomal accumulation of charged
421 phospholipids, an effect that has been reported for many CADs (8, 45). DIPL shows
422 morphological resemblance of Niemann-Pick type C disease (NPC-1), an inherited
423 and generally fatal lipid-storage disorder, and similar diseases (8, 46). Amiodarone
424 preferentially accumulates in the lung, causes DIPL and is associated with lung
425 dysfunction (47). However, the CADs in clinical use have not been linked to
426 Niemann-Pick like symptoms and a clear general link between cellular DIPL and
427 organ toxicity has not been demonstrated. Moreover, tissue accumulation seems to
428 be reversible within a few days (48). Nevertheless, DIPL is considered a concern in
429 drug development. In our study, we found that DIPL strongly correlates with both
430 antiviral activity and with hydrophobicity. However, visible DIPL itself is not required
431 for antiviral activity of CADs since effects like EBOV VLP inhibition (32) or lysosomal
432 calcium flux changes (49) precede DIPL induction for hours. In conclusion, DIPL
433 induction seems to be more prominent among CADs with antiviral activity. In fact, in
434 our series all CADs with antiviral activity also induce DIPL to some extent. Yet, the

ability to induce DIPL is not the only determinant of antiviral activity, as some CADs with similar DIPL values have quite different degrees of antiviral activity.

Filoviruses are late-penetrating viruses that are taken up into endosomes following low-specificity interactions with one or more of various cell surface attachment factors (34). Within the endosome, they undergo gp priming by low-pH dependent cathepsin and interact with their endolysosomal receptor NPC1, a cholesterol transporter (50). This enables membrane fusion, thereby releasing the nucleocapsid into the cytosol (51, 52). It is conceivable that CADs modulate endosomal or endolysosomal membranes or membrane-attached proteins in a manner that perturbs viral penetration. Direct evidence or a clear concept of how this might occur is as yet lacking. So far, it has not even been fully established whether CADs exert their antiviral effects on the host cell or the viral particle. It has been reported for a group of structurally diverse EBOV-inhibiting CADs – of which toremifen, bepridil, and sertraline were tested in our study – that these compounds decrease the overall stability of the GP1-GP2 dimers, thus inhibiting fusion (53, 54). Another recent study described that the CAD flunarizine as well as the structurally similar fluphenazine, trifluoperazine, chlorcyclizine and chlorpromazine seem to inhibit membrane fusion of HCV particles by targeting a specific hydrophobic region in the E1 protein (16, 55). Moreover, the antiviral spectrum of amiodarone, bepridil, amodiaquine and raloxifene together with lipid mixing assays suggest that mostly late penetrating viruses and a late entry step, most probably membrane fusion, are affected by these CADs (22).

However, given that we and others have described a range of structurally diverse CADs as inhibitors of cell entry by different unrelated virus species it seems likely that besides these virus-specific effects there is a shared mechanism common to diverse CADs affecting a range of enveloped viruses. The correlation of antiviral effects and early events of DIPL points towards a cell-based effect of CADs that takes place in

the endolysosomal compartment. Thus, we consider that the perturbation of late endosomal homeostasis might be the underlying antiviral mechanism of CADs. The clearer elucidation of the antiviral mechanism of some CADs is part of an ongoing follow-up study.

In summary, we describe the most comprehensive evaluation to date of the antiviral properties among CADs and show how antiviral activity is linked to structural features. Most notably, we show that antiviral activity is strongly associated with hydrophobicity and DIPL induction in target cells, corroborating previous studies (32). Overall, our findings help clarify the structure-activity relationship of antiviral CADs. Furthermore, using an *in silico* screening approach for identification of structurally and functionally related compounds, we identified novel CADs with antiviral properties. By showing that CAD-antiviral activity is partially fingerprinted on their molecular architecture, we set a basis for the structure-based design of potent antiviral CADs.

5. Acknowledgements

We thank Petra Schneider (ETH, Pharmaceutical Sciences, Zürich, Switzerland) for help with CATS software, Barbara Hertel (University of Potsdam, Department for food chemistry, Potsdam, Germany) for excellent experimental support and Beate Sodeik (MHH, Institute of Virology, Hannover, Germany) for helpful discussions.

6. Funding

This work was supported by Deutsches Zentrum für Infektionsforschung (DZIF, German Center for Infection Research; grant number 05807) and German Research Foundation (DFG) via SFB738 (Research Project B2). AG is PhD student of ZIB and HBRS.

7. Declaration of interests

None.

8. References

1. WHO. 2019. WHO-Disease Outbreak News. Available at: https://www.who.int/csr/don/en/ (Accessed 2019-09-02)
2. Coltart CEM, Lindsey B, Ghinai I, Johnson AM, Heymann DL. 2017. The Ebola outbreak , 2013 – 2016 : old lessons for new epidemics. Philos Trans R Soc Lond B Biol Sci 372:1–24.
3. Shaffer JG, Grant DS, Schieffelin JS, Boisen ML, Goba A, Hartnett JN, Levy DC, Yenni RE, Moses LM, Fullah M, Momoh M, Fonnie M, Fonnie R, Kanneh L, Koroma VJ, Kargbo K, Ottomassathien D, Muncy IJ, Jones AB, Illick MM, Kulakosky PC, Haislip AM, Bishop CM, Elliot DH, Brown BL, Zhu H, Hastie KM, Andersen KG, Gire SK, Tabrizi S, Tariyal R, Stremlau M, Matschiner A, Sampey DB, Spence JS, Cross RW, Geisbert JB, Folarin OA, Happi CT, Pitts KR, Geske FJ, Geisbert TW, Saphire EO, Robinson JE, Wilson RB, Sabeti PC, Henderson LA, Khan SH, Bausch DG, Branco LM, Garry RF. 2014. Lassa Fever in Post-Conflict Sierra Leone. PLoS Negl Trop Dis 8:1–13.

4. WHO. 2018. 2018 Annual review of diseases prioritized under the Research and Development Blueprint.
5. Martinez JP, Sasse F, Brönstrup M, Diez J, Meyerhans A. 2015. Antiviral drug discovery: Broad-spectrum drugs from nature. Nat Prod Rep 32:29–48.
6. Bekerman E, Einav S. 2015. Combating emerging viral threats. Science (80-) 348:282–283.
7. Reasor MJ, Hastings KL, Ulrich RG. 2006. Drug-induced phospholipidosis: issues and future directions. Expert Opin Drug Saf 5:567–83.
8. Lüllmann H, Lüllmann-Rauch R, Wassermann O. 1978. Lipidosis induced by amphiphilic cationic drugs. Biochem Pharmacol 27:1103–1108.
9. Morissette G, Ammoury A, Rusu D, Marguery MC, Lodge R, Poubelle PE, Marceau F. 2009. Intracellular sequestration of amiodarone: Role of vacuolar ATPase and macroautophagic transition of the resulting vacuolar cytopathology. Br J Pharmacol 157:1531–1540.
10. Kazmi F, Hensley T, Pope C, Funk RS, Loewen GJ, Buckley DB, Parkinson A. 2013. Lysosomal sequestration (trapping) of lipophilic amine (cationic amphiphilic) drugs in immortalized human hepatocytes (Fa2N-4 cells). Drug Metab Dispos 41:897–905.
11. Gehring G, Rohrmann K, Atenchong N, Mittler E, Becker S, Dahlmann F, Pöhlmann S, Vondran FWR, David S, Manns MP, Ciesek S, von Hahn T. 2014. The clinically approved drugs amiodarone, dronedarone and verapamil inhibit filovirus cell entry. J Antimicrob Chemother 69:2123–2131.
12. Johansen LM, Brannan JM, Delos SE, Shoemaker CJ, Stossel A, Lear C, Hoffstrom BG, DeWald LE, Schornberg KL, Scully C, Lehar J, Hensley LE, White JM, Olinger GG. 2013. FDA-Approved Selective Estrogen Receptor Modulators Inhibit Ebola Virus Infection. Sci Transl Med 5:190ra79-190ra79.

13. Klintworth A, Nolden T, Westhaus S, Rohrmann K, David S, Manns MP, Finke S, Ciesek S, von Hahn T. 2015. Cationic amphiphilic drugs enhance entry of lentiviral particles pseudotyped with rabies virus glycoprotein into non-neuronal cells. Antiviral Res 124:122–31.

14. Cheng Y-L, Lan K-H, Lee W-P, Tseng S-H, Hung L-R, Lin H-C, Lee F-Y, Lee S-D, Lan K-H. 2013. Amiodarone inhibits the entry and assembly steps of hepatitis C virus life cycle. Clin Sci 125:439–448.

15. Gastaminza P, Whitten-Bauer C, Chisari F V. 2010. Unbiased probing of the entire hepatitis C virus life cycle identifies clinical compounds that target multiple aspects of the infection. Proc Natl Acad Sci 107:291–296.

16. Perin PM, Haid S, Brown RJP, Doerrbecker J, Schulze K, Zeilinger C, Schaewen M Von, Heller B, Vercauteren K, Baktash YM, Vondran FWR, Speerstra S, Awadh A, Mukhtarov F, Schang LM, Kirschning A, Ploss A, Pietschmann T. 2017. Flunarizine Prevents Hepatitis C Virus Membrane Fusion in a Genotype-dependent Manner by Targeting the Potential Fusion Peptide within E1. Hepatology 63:49–62.

17. Owens CM, Mawhinney C, Grenier JM, Altmeyer R, Lee MS, Borisy AA, Leha J, Johansen LM. 2010. Chemical combinations elucidate pathway interactions and regulation relevant to Hepatitis C replication. Mol Syst Biol 6:1–13.

18. He S, Lin B, Chu V, Hu Z, Hu X, Xiao J, Wang AQ, Schweitzer CJ, Li Q, Imamura M, Hiraga N, Southall N, Ferrer M, Zheng W, Chayama K, Marugan JJ, Liang TJ. 2015. Repurposing of the antihistamine chlorcyclizine and related compounds for treatment of hepatitis C virus infection. Sci Transl Med 7:1–10.

19. Nawa M, Takasaki T, Yamada KI, Kurane I, Akatsuka T. 2003. Interference in Japanese encephalitis virus infection of Vero cells by a cationic amphiphilic drug, chlorpromazine. J Gen Virol 84:1737–1741.

556 20. Stadler K, Ha HR, Ciminale V, Spirli C, Saletti G, Schiavon M, Bruttomesso D,
557 Bigler L, Follath F, Pettenazzo A, Baritussio A. 2008. Amiodarone alters late
558 endosomes and inhibits SARS coronavirus infection at a post-endosomal level.
559 Am J Respir Cell Mol Biol 39:142–149.
560 21. Nemerow GR, Cooper NR, Muller-Eberhard HJ. 1984. Infection of B
561 lymphocytes by a human herpesvirus, Epstein-Barr virus, is blocked by
562 calmodulin antagonists. Med Sci 81:4955–4959.
563 22. Mazzon M, Ortega-Prieto AM, Imrie D, Luft C, Hess L, Czieso S, Grove J,
564 Skelton JK, Farleigh L, Bugert JJ, Wright E, Temperton N, Angell R, Oxenford
565 S, Jacobs M, Ketteler R, Dorner M, Marsh M. 2019. Identification of Broad-
566 Spectrum Antiviral Compounds by Targeting Viral Entry. Viruses 11:1–26.
567 23. Kutner RH, Zhang XY, Reiser J. 2009. Production, concentration and titration
568 of pseudotyped HIV-1-based lentiviral vectors. Nat Protoc 4:495–505.
569 24. Ciesek S, Westhaus S, Wicht M, Wappler I, Henschen S, Sarrazin C, Hamdi N,
570 Abdelaziz AI, Strassburg CP, Wedemeyer H, Manns MP, Pietschmann T, von
571 Hahn T. 2011. Impact of Intra- and Interspecies Variation of Occludin on Its
572 Function as Coreceptor for Authentic Hepatitis C Virus Particles0. J Virol
573 85:7613–7621.
574 25. Flint M, von Hahn T, Zhang J, Farquhar M, Jones CT, Balfe P, Rice CM,
575 McKeating JA. 2006. Diverse CD81 Proteins Support Hepatitis C Virus
576 Infection. J Virol 80:11331–11342.
577 26. Mittler E, Kolesnikova L, Strecker T, Garten W, Becker S. 2007. Role of the
578 Transmembrane Domain of Marburg Virus Surface Protein GP in Assembly of
579 the Viral Envelope. J Virol 81:3942–3948.
580 27. Chemical Abstracts Service. 2017. SciFinder. Columbus OH.
581 28. Schneider G, Neidhart W, Giller T, Schmid G. 1999. “Scaffold-Hopping” by

topological pharmacophore search: A contribution to virtual screening. Angew Chemie - Int Ed 38:2894–2896.

29. Madrid PB, Panchal RG, Warren TK, Shurtle AC, Endsley AN, Green CE, Kolokoltsov A, Davey ΔR, Manger ΠID, Gil L, Bavari S, Tanga MJ. 2015. Evaluation of Ebola Virus Inhibitors for Drug Repurposing. ACS Infect Dis 1:317–326.

30. Salata C, Baritussio A, Munegato D, Calistri A, Ha HR, Bigler L, Fabris F, Parolin C, Palù G, Mirazimi A. 2015. Amiodarone and metabolite MDEA inhibit Ebola virus infection by interfering with the viral entry process. Pathog Dis 73:1–9.

31. Chockalingam K, Simeon RL, Rice CM, Chen Z. 2010. A cell protection screen reveals potent inhibitors of multiple stages of the hepatitis C virus life cycle. Proc Natl Acad Sci 107:3764–3769.

32. Shoemaker CJ, Schornberg KL, Delos SE, Scully C, Pajouhesh H, Olinger GG, Johansen LM, White JM. 2013. Multiple Cationic Amphiphiles Induce a Niemann-Pick C Phenotype and Inhibit Ebola Virus Entry and Infection. PLoS One 8:1–13.

33. Johansen LM, Dewald LE, Shoemaker CJ, Hoffstrom BG, Lear-rooney CM, Stossel A, Nelson E, Delos SE, Simmons JA, Grenier JM, Pierce LT, Pajouhesh H, Lehár J, Hensley LE, Glass PJ, White JM, Olinger GG. 2015. A screen of approved drugs and molecular probes identifies therapeutics with anti – Ebola virus activity. Sci Transl Med 7:1–14.

34. Zapatero-Belinchón FJ, Dietzel E, Dolnik O, Döhner K, Costa R, Hertel B, Veselkova B, Kirui J, Klintworth A, Manns MP, Pöhlmann S, Pietschmann T, Krey T, Ciesek S, Gerold G, Sodeik B, Becker S, von Hahn T. 2019. Characterization of the Filovirus-Resistant Cell Line SH-SY5Y Reveals

608 Redundant Role of Cell Surface Entry Factors. Viruses 11:1–26.
609 35. Wool-Lewis RJ, Bates P. 1998. Characterization of Ebola Virus Entry by Using
610 Pseudotyped Viruses: Identification of Receptor-Deficient Cell Lines. J Virol
611 72:3155–3160.
612 36. Holt DW, Tucker GT, Jackson PR, Storey GCA. 1983. Amiodarone
613 pharmacokinetics. Am Heart J 106:840–847.
614 37. Goldschlager N, Epstein A, Naccarelli G, Olshansky B, Singh B. 2000. Practical
615 guidelines for clinicians who treat patients with amidoarone. Arch Intern Med
616 160:1741–1748.
617 38. Reis M, Åberg-Wistedt A, Ågren H, Höglund P, Åkerblad AC, Bengtsson F.
618 2004. Serum disposition of sertraline, N-desmethylsertraline and paroxetine: A
619 pharmacokinetic evaluation of repeated drug concentration measurements
620 during 6 months of treatment for major depression. Hum Psychopharmacol
621 19:283–291.
622 39. Sanofi-Aventis Deutschland GmbH. 2011. Fachinformation (prescription
623 information for physicians) MULTAQ.
624 40. Drayer DE. 1984. Clinical Consequences of the Lipophilicity and Plasma
625 Protein Binding of Antiarrhythmic Drugs and Active Metabolites in Man. Ann N
626 Y Acad Sci 432:45–56.
627 41. Ghose AK, Pritchett A, Crippen GM. 1988. Atomic Physicochemical
628 Parameters for 3D-QSAR III: Modeling Hydrophobic Interactions Relationships.
629 JComputChem 9:80–90.
630 42. Reutlinger M, Koch CP, Reker D, Todoroff N, Schneider P, Rodrigues T,
631 Schneider G. 2013. Chemically Advanced Template Search (CATS) for
632 Scaffold-Hopping and Prospective Target Prediction for ‘Orphan’ Molecules.
633 Mol Inform 32:133–138.

634 43. Ploemen J-PHTM, Kelder J, Hafmans T, van de Sandt H, van Burgsteden JA,
635 Salemink PJM, van Esch E. 2004. Use of physicochemical calculation of pKa
636 and CLogP to predict phospholipidosis-inducing potential. Exp Toxicol Pathol
637 55:347–355.
638 44. Pelletier DJ, Gehlhaar D, Tilloy-Ellul A, Johnson TO, Greene N. 2007.
639 Evaluation of a published in silico model and construction of a novel Bayesian
640 model for predicting phospholipidosis inducing potential. J Chem Inf Model
641 47:1196–1205.
642 45. Halliwell WH. 1997. Cationic Amphiphilic Drug-induced Phospholipidosis.
643 Toxicol Pathol 25:53–60.
644 46. Adams PC, Holt DW, Storey GCA, Morley AR, Callaghan J, Campbell RW.
645 1985. Amiodarone and its desethyl metabolite: Tissue distribution and
646 morphologic changes during long-term therapy. Circulation 72:1064–1075.
647 47. Kodavanti U, Mehendale HM. 1990. Cationic Amphiphilic Drugs and
648 Phospholipid Storage Disorder *. Pharmacol Rev 42:327–354.
649 48. McCloud CM, Beard TL, Kacew S, Reasor MJ. 1995. In vivo and in vitro
650 reversibility of chlorphentermine-induced phospholipidosis in rat alveolar
651 macrophages. Exp Mol Pathol 62:12–21.
652 49. Lloyd-Evans E, Morgan AJ, He X, Smith DA, Elliot-Smith E, Sillence DJ,
653 Churchill GC, Schuchman EH, Galione A, Platt FM. 2008. Niemann-Pick
654 disease type C1 is a sphingosine storage disease that causes deregulation of
655 lysosomal calcium. Nat Med 14:1247–55.
656 50. Côté M, Misasi J, Ren T, Bruchez A, Lee K, Filone CM, Hensley L, Li Q, Ory D,
657 Chandran K, Cunningham J. 2011. Small molecule inhibitors reveal Niemann-
658 Pick C1 is essential for Ebola virus infection. Nature 477:344–8.
659 51. Simmons JA, Ruas M, Galione A, Casanova JE, White JM. 2016. Ebolavirus

660 Glycoprotein Directs Fusion through NPC1+ Endolysosomes. J Virol 90:605–
661 610.
662 52. Mingo RM, Simmons JA, Shoemaker CJ, Nelson EA, Schornberg KL, D'Souza
663 RS, Casanova JE, White JM. 2015. Ebola Virus and Severe Acute Respiratory
664 Syndrome Coronavirus Display Late Cell Entry Kinetics: Evidence that
665 Transport to NPC1 $^{+}$ Endolysosomes Is a Rate-Defining Step. J Virol 89:2931–
666 2943.
667 53. Zhao Y, Ren J, Harlos K, Jones DM, Zeltina A, Bowden TA, Padilla-Parra S,
668 Fry EE, Stuart DI. 2016. Toremifene interacts with and destabilizes the Ebola
669 virus glycoprotein. Nature 535:169–172.
670 54. Ren J, Zhao Y, Fry EE, Stuart DI. 2018. Target Identification and Mode of
671 Action of Four Chemically Divergent Drugs against Ebolavirus Infection. J Med
672 Chem 61:724–733.
673 55. Banda DH, Perin PM, Brown RJP, Todt D, Solodenko W, Hoffmeyer P, Sahu
674 KK, Houghton M, Meuleman P, Müller R, Kirschning A, Pietschmann T. 2019.
675 A central hydrophobic E1 region controls the pH range of hepatitis C virus
676 membrane fusion and susceptibility to fusion inhibitors. J Hepatol 70:1082–
677 1092.
678
679 **Table 1: Cationic amphiphilic drugs included in single-point assay and their**
680 **properties.**

	Compound name	Drug class	pK_a	ClogP	Molecular weight [g/mol]
1	Fenfluramine HCl	Anorexic	10.22	3.36	267.72
2	Clemastine fumarate salt	Antiallergic	9.55	5.2	459.96

3	Perhexiline maleate salt	Antianginal	10.58	6.2	393.56
4	Bepridil HCl	Antianginal	9.16	5.49	403
5	Dronedarone HCl	Antiarrhythmic	9.08	5.28	593.22
6	Propranolol HCl	Antiarrhythmic	9.67	3.48	295.8
7	Verapamil HCl	Antiarrhythmic	9.68	5.04	491.06
8	Amiodarone HCl	Antiarrhythmic	8.47	7.64	681.77
9	Gentamicin sulfate	Antibiotic	10.18	-3.1	516.604
10	Teicoplanin	Antibiotic	7.1	-3.71	1879.7
11	Sertraline HCl	Antidepressant	9.85	5.1	342.69
12	N-Desethylamiodarone HCl solution	Antidepressant	9.4	6.27	653.72
13	Clomipramine HCl	Antidepressant	9.2	5.19	351.31
14	Fluoxetine HCl	Antidepressant	9.8	4.09	345.79
15	Imipramine HCl	Antidepressant	9.2	4.8	316.87
16	Maprotiline HCl	Antidepressant	10.54	5.1	313.86
17	Mianserin HCl	Antidepressant	6.92	3.52	300.83
18	Zimelidine Dihydrochloride	Antidepressant	8.62	3.39	390.15
19	Cyclizine HCl	Antiemetic	8.51	3	302.84
20	Amorolfine HCl	Antifungal	7.1	6.4	353.97
21	Terconazole	Antifungal	8.8	4.8	532.46
22	Thioridazine HCL	Antifungal	8.8	4.8	407.04
23	Promethazine HCl	Antihistaminic	9.05	4.81	320.88
24	Tripelennamine HCl	Antihistaminic	8.76	3.3	291.82
25	Chlorcyclizine	Antihistaminic	8	4.15	300.83
26	Quinacrine dihydrochloride	Antiprotozoal	10.33	5.5	472.88

27	Chloroquine Diphosphate salt	Antiprotozoal	10.32	4.63	515.86
28	Promazine HCl	Antipsychotic	9.4	4.55	320.88
29	Clorpromazine HCl	Antipsychotic	9.35	5.41	355.33
30	Prochlorperazine dimaleate salt	Antipsychotic	8.39	4.88	606.09
31	Flupentixol dihydrochloride	Antipsychotic	8.51	4.51	507.44
32	Trifluoperazine HCl	Antipsychotic	8.39	5.03	480.42
33	Clozapine	Antipsychotic	7.35	3.23	326.82
34	Fluphenazine dihydrochloride	Antipsychotic	8.21	4.36	510.44
35	Amantadine HCl	Antiviral	10.71	2.53	187.71
36	Clomiphene citrate salt	Hormone analogue	9.31	6.47	598.08
37	Enclomiphene HCl	Hormone analogue	9.31	6.47	442.42
38	Ro 48-8071	Lipid lowering	8.8	5.7	448.4
39	Triparanol	Lipid lowering	9.6	6.7	438
40	W-5 HCl	Non-clinical	10.3	2.9	342.88
41	U18666A	Non-clinical	9.7	5.1	424.06
42	Benzylamine	Non-clinical	9.51	1.1	107.15
43	W-7	Non-clinical	10.3	3.8	377.33
44	Dasatinib	Antineoplastic	8.49	1.8	488.01
45	Toremifene Citrate salt	Antineoplastic	8.76	6.8	598.08

681

682

683

684

685 **Table 2: Antiviral activity (IC_{50}) and toxicity (CC_{50}) as well as selective indices**

686 **of top and bottom antiviral CADs.**

Antiviral effect	Compund name	IC_{50} [µM]	CC_{50} [µM]	SI
Top antiviral CADs	**Dronedarone**	1.3	13.2	10
	Triparanol	2.0	25.1	13
	Sertraline	2.9	18.7	6
	Amiodarone	1.6	54.0	34
	Perhexiline	2.4	13.8	6
	Clomifene	2.7	44.8	17
Bottom antiviral CADs	**Promazine**	29.3	51.6	2

687

688

689

690 **Figure 1: Antiviral activity against MARVpp gp-drven cell entry and cytotoxicity**
691 **of 45 CADs.** (a) EA.hy926 target cells were transduced with MARVpp encoding an
692 NLuc reporter gene in a single-point approach in the presence of various CADs at 5
693 µM. Results were normalised to solvent control. (b) Cytotoxic and antiproliferative
694 effects were evaluated for CADs at 5 µM in EA.hy926 cells stably expressing Nluc.
695 Box-whiskers plots show the median, interquartile range and standard deviation of
696 n=3 independent experiments. Asterisks indicate statistical significance of differences
697 between compounds and solvent control that was calculated by One-way ANOVA
698 with correction for multiple comparisons. (*p<0.01; **p<0.001;***p<0.0001)

699

700 **Figure 2: Correlation of MARVpp antiviral activity of 45 CADs and their**
701 **physico-chemical properties.**
702 Residual transductoin of 45 CADs against MARVpp gp-driven cell entry of single-
703 point assays were normalised and the average of n=3 independent experiments was
704 correlated with (a) pKa, (b) ClogP, (c) molecular weight and (d) linker length of all
705 tested CADs. The prototypical CAD amiodarone is labelled. Non-parametric
706 Spearman-correlation was computed and the correlation coefficient R and p-value
707 represent statistical significance (ns: $p > 0.12$; *$p < 0.03$; **$p < 0.002$; ***$p < 0.0002$;
708 ****$p < 0.0001$).

709

710 **Figure 3: Correlation of MARVpp antiviral activity, DIPL induction and**
711 **hydrophobicity.**
712 (a) EA.hy926 cells were treated in triplicate with 16 different CADs at a 5 µM
713 concentration and the fluorescent phospholipid LipidTox™ Green (1:1). After 6 h
714 incubation, medium was exchanged and compounds (without LipidTox™) were

715 added again for extra 18 h. Fluorescence measured by FACS represents DIPL
716 induction by CADs. Delta mean fluorescence intensity (ΔMFI) was calculated by first
717 substracting the average solvent control from single values. Averages of n=3
718 independent stainings were calculated and plotted against average antiviral activity.
719 (b) DIPL induction was correlated with ClogP of the investigated 16 CADs.
720 Correlation coefficients R were determined via Spearman-correlation (ns: $p > 0.12$;
721 *$p < 0.03$; **$p < 0.002$; ***$p < 0.0002$; ****$p < 0.0001$).
722
723 **Figure 4: Antiviral activity and cytotoxicity of dronedarone structural**
724 **derivatives.**
725 Dronedarone-derivatives D-1 and D-2 were found by SciFinder® similarity search
726 and applied in a 5 µM concentration (a) together with MARVpp on EA.hy926 cells or
727 (b) on EA.hy-NLuc cells for 6 h. Luciferase activity was determined after 72 h.p.t. and
728 triplicate values of n=3 independent experiments were normalised to solvent control.
729 Statistical difference was calculated by One-way ANOVA corrected for multiple
730 comparisons and is represented by asterisks (*$p<0.01$; **$p<0.001$;***$p<0.0001$).
731
732 **Figure 5: Inhibition of MARVpp gp-mediated cell entry and cytotoxicity of**
733 **additional CADs identified by CATS analysis.**
734 New CADs were identified in a CATS-screen for compounds with similar chemical
735 properties to seed compounds. Eight double hits were chosen which fitted the
736 requirements of being a CAD, having diverse functional groups, and having ClogP
737 > 4. In order to simplify compound nomenclature, new CADs were abbreviated
738 according to the initials of their two seed compounds. (a) For analysis of viral entry
739 inhibition, 5 µM CADs were applied together with MARVpp on EA.hy926 cells and
740 luciferase activity was measured in transduced cells 72 h.p.t. (b) Cytotoxicity of new

741 CADs, seed compounds and solvent controls was measured in EA.hy-NLuc cells
742 treated with 5 µM CADs for 6 h. Normalised results of n=3 experiments with three
743 technical replicates are shown and asterisks indicate statistical significance to solvent
744 control calculated by One-way ANOVA including multiple comparisons test. (*p<0.01;
745 **p<0.001;***p<0.0001)

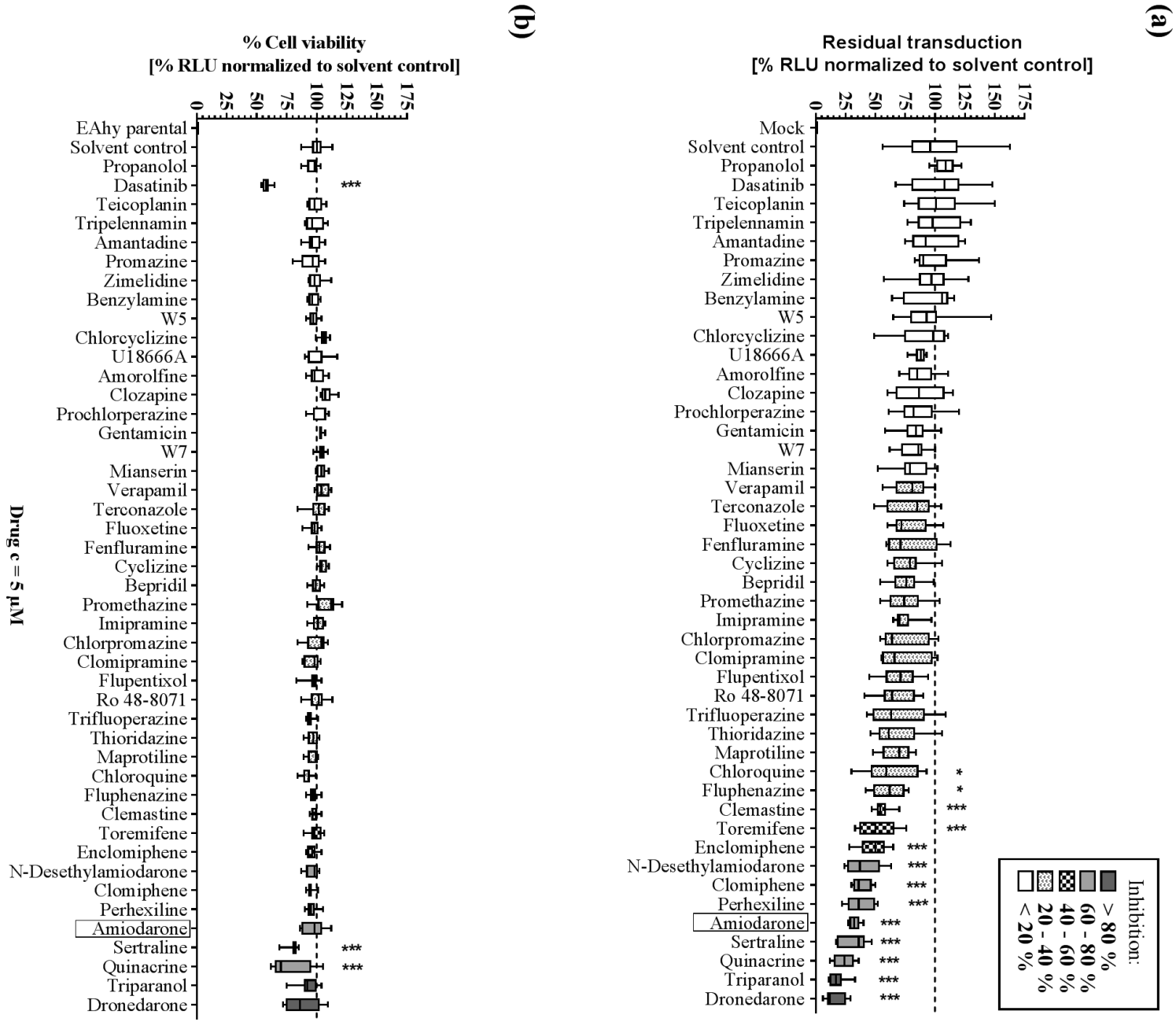

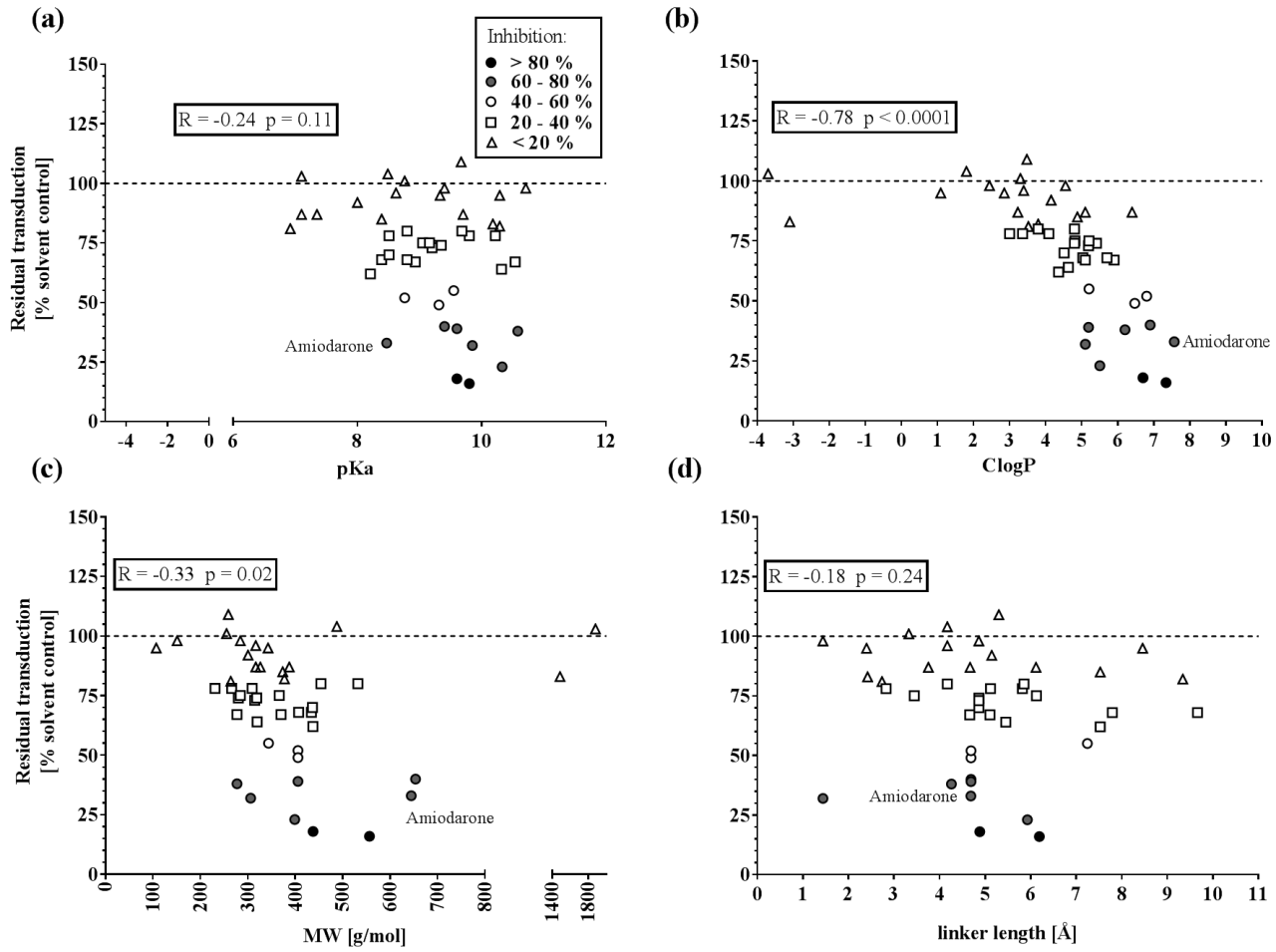

Antimicrobial Agents and Chemotherapy